X-641-71-155

NASA TM X- 65584

TRAPPED-PARTICLE RADIATION ENCOUNTERED BY SELECTED LOW-ALTITUDE SKYLAB MISSIONS: SPACE STATIONS IN AN AMBIENT RADIATION ENVIRONMENT

E. G. STASSINOPOULOS

APRIL 1971

GSFC
GODDARD SPACE FLIGHT CENTER
GREENBELT, MARYLAND

X-641-71-155

TRAPPED-PARTICLE RADIATION ENCOUNTERED BY SELECTED LOW-ALTITUDE SKYLAB MISSIONS: SPACE STATIONS IN AN AMBIENT RADIATION ENVIRONMENT

A Special Study Conducted for the
Office of Manned Space Flight
NASA-Headquarters

by

E. G. Stassinopoulos

NASA-Goddard Space Flight Center
Space Sciences Directorate
Laboratory for Space Physics
Theoretical Studies Branch

April 1971

GODDARD SPACE FLIGHT CENTER
Greenbelt, Maryland

CONTENTS

TRAPPED-PARTICLE RADIATION ENCOUNTERED BY SELECTED LOW-ALTITUDE SKYLAB MISSIONS: SPACE STATIONS IN AN AMBIENT RADIATION ENVIRONMENT

Foreword:

At the request of The Office of Manned Space Flight/Code MT, and in order to supply the Office with necessary data and information that would enable decisions to be made about the "Space Platform" program during the early planning stages of the mission, a special radiation study was conducted for a series of selected trajectories.

This report contains the results of our study; it presents an analysis of the data obtained with interpretive comments and evaluations, including all pertinent background information and explanations.

Trajectory Generation and Conversion:

For the specified flight-paths, orbit tapes were generated from the latest ephemerides, taking into account normal perturbations (drag, radiation pressure, planetary and lunar perturbations) wherever applicable, with an integration step-size of one minute, in all cases.

Each trajectory was generated for a sufficiently long flight-time so as to insure an adequate sampling of the ambient environment; on account of their period, which determines the orbit-precession, the following circular flight paths of 48-hour duration were produced:

h =	i = 28°	52°	65°	72°
278 km		x	x	x
370 km	x	x	x	x
463 km		x	x	x
556 km	x	x	x	x

The orbits were subsequently converted from geocentric polar into magnetic B/L coordinates with McIlwain's INVAR program of 1965, utilizing the GSFC (12,/1966) geomagnetic field model by Cain et al., calculated for the epoch

1971.0, where B is the field strength and L is the geocentric distance to the intersect of the field line with the geomagnetic equator.

A circular trajectory with high inclination ($i > 55°$) traverses the terrestrial radiation belts twice during each revolution. The vehicle thus executes a transverse motion in L-space, passing successively through a region of low L-values ($1.0 \lesssim L \lesssim 2.0$) and of high L-values ($2.0 \lesssim L \lesssim 6.6$), commonly referred to as the inner zone and the outer zone.

Models of the Trapped Particle Environment and Temporal Variations:

Orbital flux integrations were performed with Vette's current environment models, the AE2 for electrons and the AP1, AP6, AP7 for high energy protons. All are static models which do not consider temporal variations. For the protons this is a valid representation because experimental measurements have shown that no significant changes with time have occurred. With the exception of the fringe areas of the proton belt, that is, at very low altitudes and at the outer edges of the trapping region, the possible error introduced by the static approximation lies well within the uncertainty factor of 2, attached to the models. Consequently, the proton models may be applied to any epoch and no updating process is needed.

The same is not true for the electrons, which are strongly time dependent, both in the inner as well as in the outer zone; especially in the case of the AE2 model, which describes the environment as it existed back in 1964, when the artificial component of the total population was predominant in the inner zone and solar minimum conditions prevailed in the outer zone. Specifically, in 1964 a large proportion of the Starfish electrons were still trapped in the belt between $L = 1.2$ and $L = 2.0$; these seem to have decayed down to natural background-levels by 1967-1968. On the other hand, between $L = 2.0$ and $L = 5.5$ the trapped particle population appears to be strongly solar cycle dependent, in a sense that an increase in solar activity towards solar maximum is expected to produce an increase in the ambient intensities due to an enhanced trapping mechanism. Thus, it is anticipated that the electron fluxes in the outer zone may have risen substantially during the years 1969-1970. A practical quantitative or qualitative treatment of this process is not available yet. In the meantime, estimates of the predicted population-increases vary within the scientific community; for a peak somewhere around $L = 3.4 \pm .2$, they range from a factor of 30 up to several hundred.

To obtain reasonable electron predictions for any epoch after 1964, when using the AE2, it is necessary to update the model data. In order to account for the change in the inner zone, the 1964 fluxes were exponentially decayed to July 1967 with experimentally measured decay constants. However, lacking suitable data,

the electron calculation could not be corrected for solar cycle variations. To partially compensate for this, the uncertainty factor attached to the results has been raised appropriately.

Units:

The results, relating to omnidirectional, vehicle encountered, integral, trapped particle fluxes, are presented in graphical and tabular form with the following unit convention:

1. Daily averages: total trajectory integrated flux averaged into: particles/cm ^{2} day

2. Totals per orbit: non-averaged, single-orbit integrated flux in: particles/cm ^{2} orbit

3. Peaks per orbit: highest orbit-encountered instantaneous flux in: particles/cm^2 sec

where 1 orbit = 1 revolution.

Uncertainties:

We wish to emphasize the fact that the data presented in this report are only approximations. We do not believe the results to be any better than a factor of 2-3 for the protons and a factor of 4-5 for the electrons. It is advisable to inform all potential users about this uncertainty in the data.

Orbit-integrated Fluxes and Spectra:

The results of our calculations are summarized in Tables 1 (electrons) and 2 (protons) for all requested orbital configurations. The spectral distribution for selected energies is additionally expressed in a percentage form, normalized to the E $>$ .5 Mev fluxes for electrons and the E $>$ 5. Mev fluxes for protons. A graphical superposition of the data is given, for comparison, in Figures 1 and 4, and the selected set of integral energies are plotted versus altitude and inclination in Figures 2, 3 for electrons and in Figures 5, 6 for protons. Classification of orbit-integrated spectra as hard or soft is relative, based on an overall evaluation of near earth space in terms of circular trajectories between equatorial and polar orbits.

On some preliminary graphs discontinuities appeared in the proton spectra. These "breaks" occurred because the complete proton environment is being described by three (formerly four) independent maps or grids, each valid only over a limited energy range; for certain critical orbital configurations the discontinuities are then produced when moving from one energy range to another. They are caused, in part, by the exponential energy parameter of the model which in many instances had to be extrapolated to make up for lacking data and, in part, to insufficient experimental measurements over some areas of B/L-space; furthermore, the discontinuities reflect the fact that the available data cannot be completely matched at their overlap. In order to overcome such spectral breaks, a continuous weighted mean curve was drawn, connecting the adjacent segments; it should be regarded as an approximate spectral distribution. In doing this, the AP1 results [30 < E (Mev) < 50] had to be totally ignored sometimes.

In Figure 1, a rise in the vehicle-encountered fluxes with height may be observed; this is typical for these altitudes. Also, for a given fixed altitude level, a clustering of the inclination curves is evident. A comparison with Figures 2 and 3 indicates a slight hardening of the spectra for higher altitudes, while an increase in inclination apparently produces a small softening effect. Both variations are marginal and may be neglected. The electron spectra may be classified as moderately hard for near earth space missions.

In Figure 4, the rise in the accumulated fluxes with altitude shows up again and the grouping effect is present. The curves indicate a substantial hardening of the spectra with an increase in height. Over the specified range of inclinations no spectral change is perceptible, but test calculations with $i = 28°$ for 556 km and 370 km produced a sizeable drop of the fluxes in the lower end of the spectrum; in addition, the 370 km orbit yielded high-energy flux-values that fell below the 52° level. Figures 5 and 6 corroborate these findings. The proton spectra may be classified as hard to very hard, in the cases where $i \rightarrow 28°$.

Attached are 24 computer plots depicting the characteristic electron and proton spectra of the twelve trajectories, individually.

Percent of Total Lifetime τ spent in the Trapped Particle Radiation Belt:

The Van Allen radiation belt extends, according to prevailing opinion and experimental evidence, to approximately synchronous altitudes along the magnetic equator, that is, to about 6.6 earth radii; there ordered particle trapping breaks down. For our purposes, we assume the stable trapping region to be bounded and well defined in conventional magnetic B/L-space. As explained before, we divide the L-range of the space into an "inner zone" ($1.1 \lesssim L \lesssim 2.0$)

and into an "outer zone" ($L \gtrsim 2.0$). Correspondingly, we will denote the percentage of total lifetime spent by the vehicle in each zone by τ^i and τ^o. The percent duration spent outside the radiation belt ($L \gtrsim 6.6$) will be given by τ^e (τ-external). For any fixed altitude and inclination $\tau^i + \tau^o + \tau^e = 100\%$.

The calculated values for τ^i, τ^o, and τ^e are presented in Table 4; they are plotted in Figure 9 versus altitude and in Figure 10 versus inclination.

It is evident from Figure 9 that the τ's are not very sensitive to changes in altitude; this holds for all tested inclinations. Because of the relatively small variations in the τ's we may eliminate altitude as a variable and use mean values of τ's instead, averaged over the altitude range specified for this study. These values are plotted in Figure 10.

As would be expected, the curves show that for low inclinations, $i < 30°$, the vehicle spends its entire lifetime in the inner zone. When inclination is raised from 30° to 50° it enters the outer zone for rapidly growing periods of time; finally, when inclination exceeds 50°, it begins leaving the trapped radiation belt, initially for short intervals of time, which however increase in almost an exponential fashion, as $i = 90°$ is approached. In this last stage the satellite performs a complete sweep through magnetic L-space, which constitutes the transverse motion mentioned earlier, executed twice during each revolution (orbit).

If additional data were available for the higher inclinations, we believe the plotted curves would continue to extend monotonically towards $i = 90°$ with the exception of the outer zone contour which indicates a folding at $i = 65°$. We would estimate the final values for a polar orbit to be approximately:

$$\tau^i = 45\%, \tau^o = 20\%, \tau^e = 35\%.$$

Because the information contained in this section may also prove useful in the selection of an orbit-inclination, we wish to bring up and submit for prior consideration the following related points:

(a) lasting solar cycle effects, that is, significant increases in the trapped electron population from solar minimum to solar maximum, are more severely experienced in the outer zone;

(b) energetic artificial electrons from high altitude nuclear explosions (Starfish) have displayed a remarkable longevity, but only in the inner zone; there, they contaminated the environment for over 5 years, while

they rapidly decayed to background levels in the outer zone (within weeks to months). A planned or accidental explosion of another atomic device with the appropriate yield and at the right latitude and altitude may, very likely, produce conditions similar to those experienced with "Starfish", transforming the inner zone again into a radiation hotbed.

Percent of Total Lifetime τ Spent in High Intensity Regions of the Van Allen Belt and Percent of Total Daily Flux Accumulated During This Time:

We arbitrarily define as "High Intensity" those regions of space, where the instantaneous, integral, omnidirectional, trapped particle flux is greater than 10^3 protons with energies $E > 5$ Mev and greater than 10^5 electrons with energies $E > .5$ Mev.

Table 3 gives the total lifetime percentage τ^{hi} for the high intensity regions and the respectively accumulated fluxes J, for protons and electrons. These values are graphically presented in Figures 7 (τ and J vs. i) and 8 (τ and J vs. h).

An interesting feature in Figure 7 is the clustering of the proton curves; evidently, the encountered high intensity proton fluxes are almost independent of inclination, while the corresponding time-curves show a substantial variation in i, which implies that the vehicle passes through regions of successively higher absolute intensities as inclination increases, but for shorter total intervals of time. This relationship seems to be more pronounced for the upper altitude levels.

A similar features appears also for the electrons at 556 kilometers. This independence is clearly expressed in Figure 8 by the zero slope of the altitude curves.

Percent of Total Lifetime τ Spent in Flux-Free Regions of Space:

In the context of this study, the term "Flux-Free" applies to all regions of space where trapped-particle intensities are less than one electron or proton per square centimeter per second, having energies $E > .5$ Mev and $E > 5$ Mev, respectively; this includes regions outside the radiation belt. We denote the percentage of mission lifetime spent in flux-free regions by τ^{ff}. Values of τ^{ff} for both types of particles are given in Table 5; they are plotted versus altitude and inclination in Figures 11 and 12, respectively.

It should be noted that the curves for protons and electrons in Figure 11 display an inverse relationship of τ^{ff} to inclination, that is, as inclination is increased the value of τ^{ff} decreases for electrons but increases for protons. This is consistent with the geomagnetic geometry of the radiation belt; it reflects the fact that the high energy (E > 5 Mev) proton population occupies a much smaller volume than the low energy (E > .5 Mev) electron population, which in addition displays the so called "horns" (Stassinopoulos, NASA SP-3054) at the altitudes under consideration. Consequently, an increase in inclination moves the trajectory farther away from the high intensity regions of the proton belt into flux-free space, but apparently it still immerses the orbit deeper into the electron belt.

A better picture of this relationship is conveyed by Figure 12. Evidently, as the inclination approaches 75° - 80°, the vehicle experiences a maximum exposure to accountable electron intensities (τ^{ff} getting smaller), whereas the proton exposure decreases continuously (τ^{ff} becomes larger), gradually levelling off to some final limiting value for a polar orbit (probably around $\tau^{ff} \approx 95\%$). It is reasonable to assume that the electrons will reverse their trend somewhere around 76° - 78° and yield possibly larger τ^{ff}'s while approaching a polar inclination.

An extension of the curves towards lower inclinations ($30° \lesssim i \lesssim 50°$) would most likely follow the pattern established in the plot. However, there is reason to believe that in the neighborhood of i = 30° a "folding" will occur for the electrons as the τ^{ff}'s slowly settle to a final limiting value for an equatorial trajectory.

Obviously, if an inclination were to be selected on the basis of τ^{ff} alone, that is, total time available in flux-free regions of space, a prior evaluation and comparison of the radiation hazards due to the predicted electron and proton fluxes would be essential, either in regards to the entire mission or in regards to specific important mission requirements. While the proton intensities are on the average two orders of magnitude smaller than the electrons, and while they afford more flux-free time for higher inclinations, their greater mass and harder spectra may prove more damaging to the mission than the more numerous electrons with their lesser flux-free time.

It appears that the dependence of τ^{ff} on altitude is almost linear for all inclinations and particles.

Peak Fluxes per Orbit:

Attached are 24 additional computer plots for the twelve initial trajectories, showing the vehicle encountered instantaneous peak electron (E > .5 Mev) and proton (E > 5. Mev) intensities per orbit for a sequence of about 30 revolutions.

On all graphs a periodic pattern emerges that indicates a daily cycle of about 15 orbits which may shift slightly, alternating between 14 and 16 orbits; this is due to the relative orbit-period, which determines the precession of the trajectory. If there were an integer number of orbit-periods in a day, then the cycle would be an exact 15 revolutions. For circular flight paths, the orbit-period is a function of the altitude. Inclination has no bearing on this process. It affects, however, the incident peak fluxes of the electrons and the protons, but apparently in different ways, as will be discussed in the next two paragraphs.

Curves of both types of particles display certain "troughs" or depressions, sometimes to the zero-flux level; usually these minima occur at the ends of the cycles and may extend over several orbits; occasionally they appear also within a cycle, as for instance in the high inclination proton plots.

In the case of our study, such intra-cyclic flux-less orbits are observed only in the proton medium and they appear to be a function of the inclination. At $i = 52°$ there is but a small depression in the top segment of the contour; at $i = 65°$ the trough has already formed, and at $i = 72°$ it is complete. It lasts for 1-2 orbits, the most, and seems to hold for all altitudes.

An increase in height raises the entire curve, thereby lifting the trough. Eventually, at some altitude the minimum will have contracted to within an order of magnitude from the top of the curve.

The inter-cyclic flux-less orbits are apparently a fundamental characteristic of the $E > 5$ Mev proton environment, that is, they show up consistently for all altitudes and inclinations. Their number varies from ~ 2 to ~ 5. The electrons demonstrate such a minimum only at the lowest inclinations considered, and only for about 1 orbit.

Time- and Flux-Histograms:

Finally, for each of the twelve flight paths, two more plots are included, one for electrons and one for protons, depicting the characteristic averaged instantaneous intensities of the trajectory in terms of constant L-bands of .1 earth radius width; the percent of total lifetime spent in each L-interval is shown on the same graph by the contour marked with the x's.

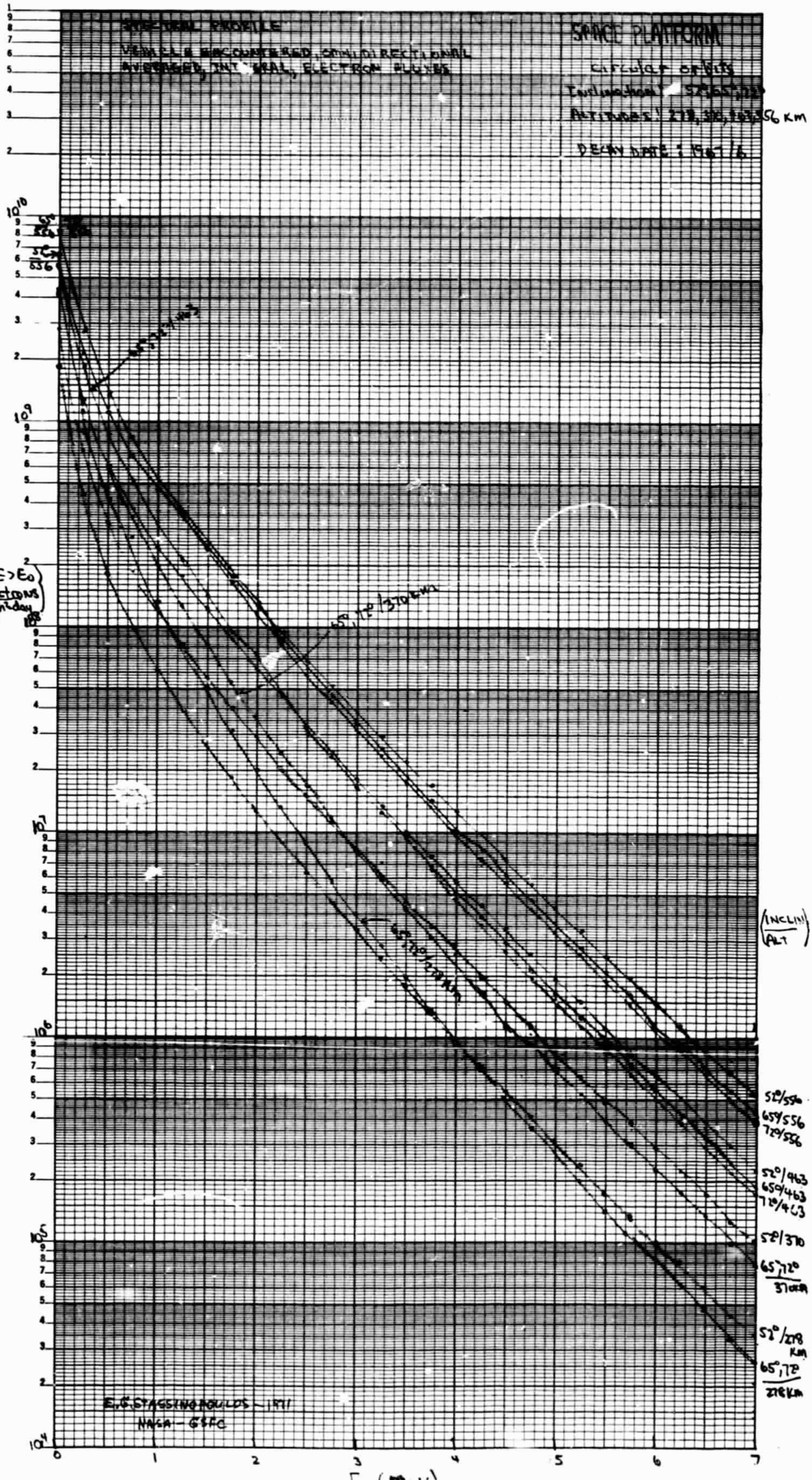
SPECTRAL PROFILE
VEHICLE ENCOUNTERED, OMNIDIRECTIONAL
AVERAGED, INTEGRAL, ELECTRON FLUXES
SPACE PLATFORM
circular orbits
Inclinations: 52°, 65°, 72°
Altitudes: 278, 370, 463, 556 km
DECAY DATE: 1967/6
J(E>Eo) (electrons / cm²-day)
Eo (MeV)
(INCLIN / ALT)
52°/556
65°/556
72°/556
52°/463
65°/463
72°/463
52°/370
65°, 72° / 370 km
52°/278 km
65°, 72° / 278 km
E. G. STASSINOPOULOS - 1971
NASA - GSFC

Figure 2

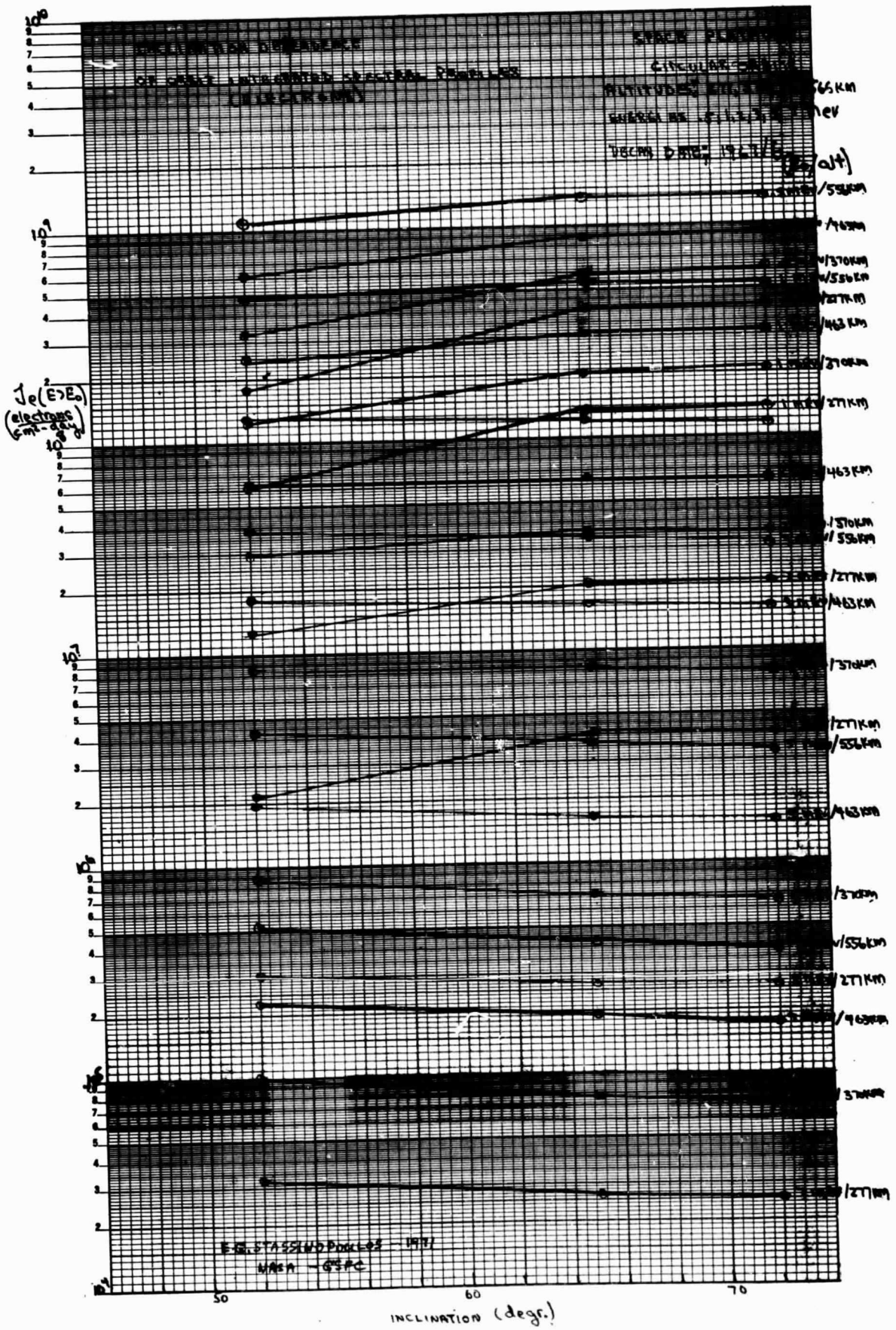

Figure 3

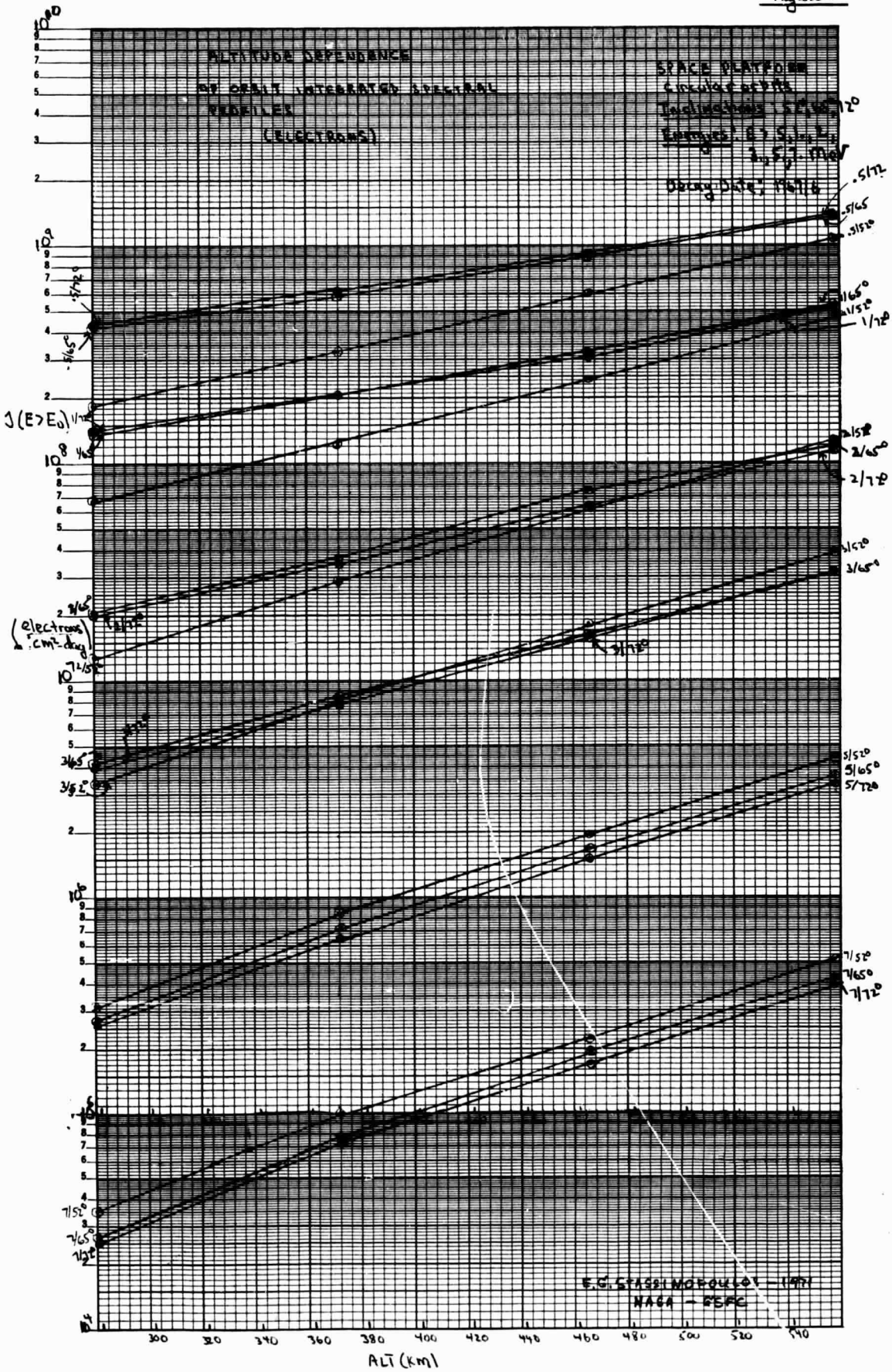
ALTITUDE DEPENDENCE
OF ORBIT INTEGRATED SPECTRAL
MODELS
(ELECTRONS)
SPACE PLATFORM
Circular orbits
Inclinations: 28°, 55°, 72°
Energies: 0.5, 1.0, 2.0 MeV
Decay Date: 1/1/76
J(E>E0) 1/cm²
(electrons/cm²-day)
ALT (km)
E.G. STASSINOPOULOS — 1977
NASA — GSFC

Figure 4

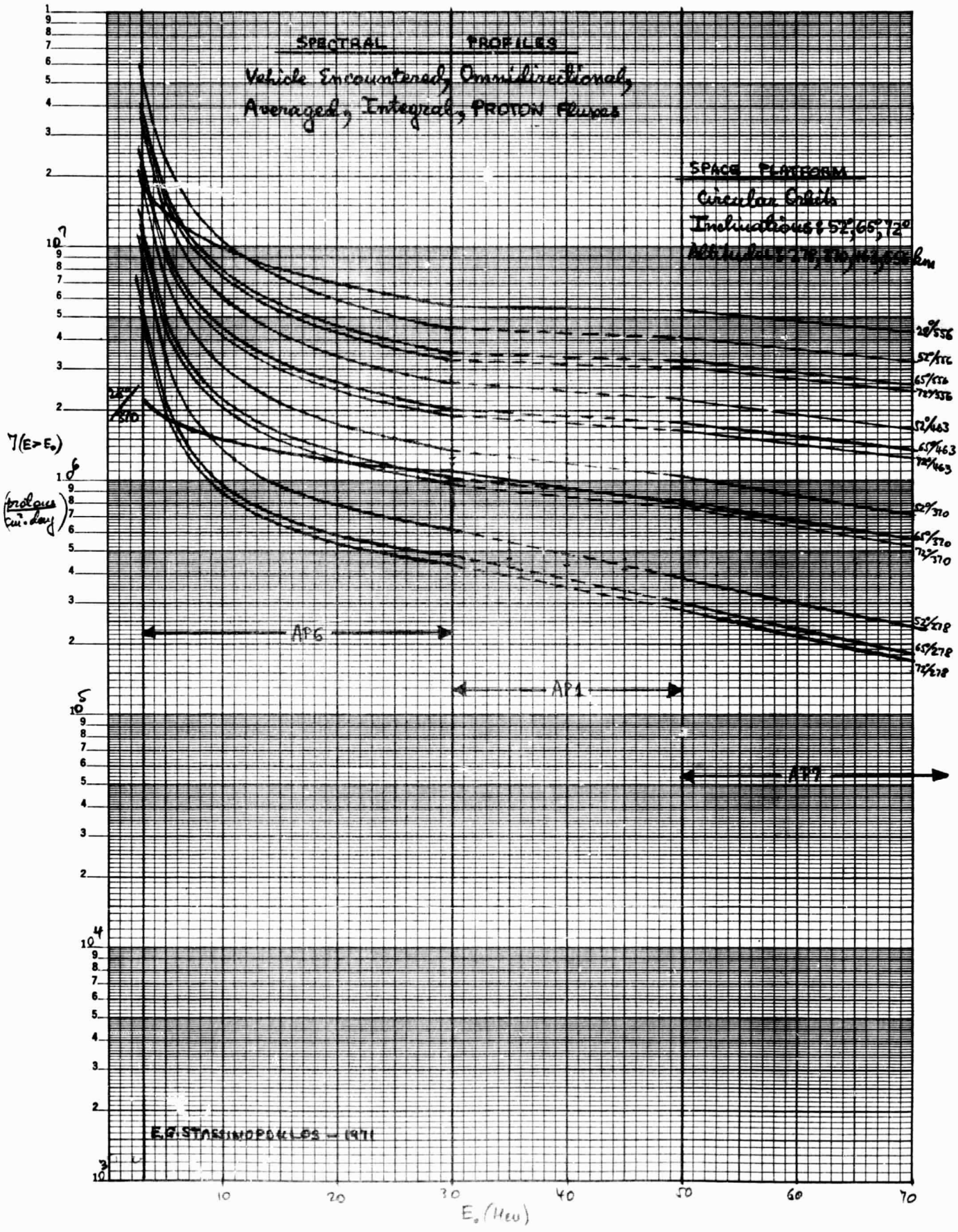
SPECTRAL PROFILES
Vehicle Encountered, Omnidirectional, Averaged, Integral, PROTON Fluxes
SPACE PLATFORM
Circular Orbits
Inclinations: 28°, 55°, 65°, 72°
Altitudes: 270, 370, 463, 556 km
28°/556
55°/556
65°/556
72°/556
28°/463
55°/463
65°/463
72°/463
28°/370
55°/370
65°/370
72°/370
28°/278
55°/278
65°/278
72°/278
AP6
AP1
AP7
N(E>E₀)
(protons/cm²-day)
E₀ (MeV)
E.G. STASSINOPOULOS — 1971

Figure 5

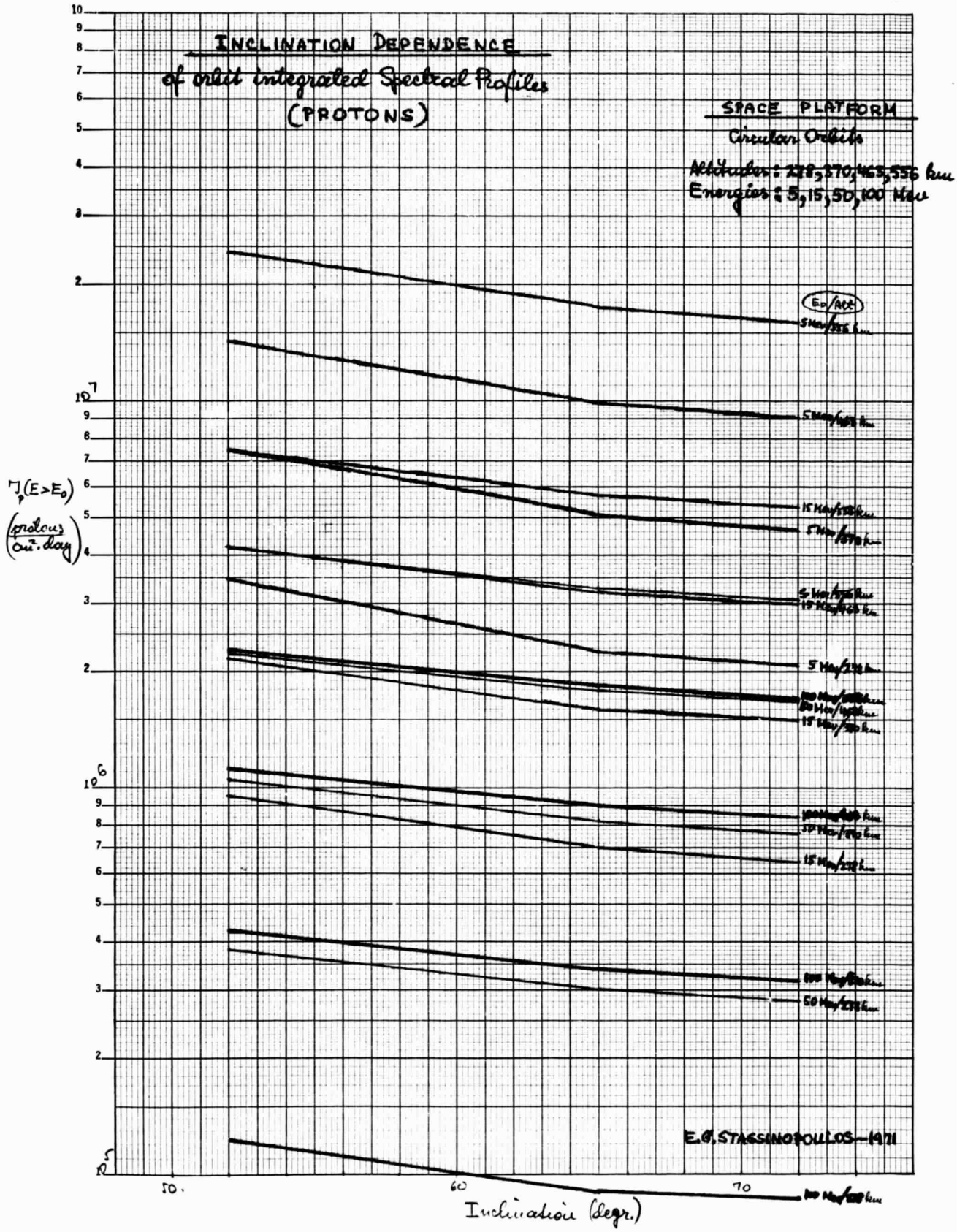
INCLINATION DEPENDENCE
of orbit integrated Spectral Profiles
(PROTONS)
SPACE PLATFORM
Circular Orbits
Altitudes: 278, 370, 463, 556 km
Energies: 5, 15, 50, 100 Mev
$J_p(E>E_0)$
(protons/cm².day)
Inclination (degr.)
E.G. STASSINOPOULOS — 1971

Figure 6

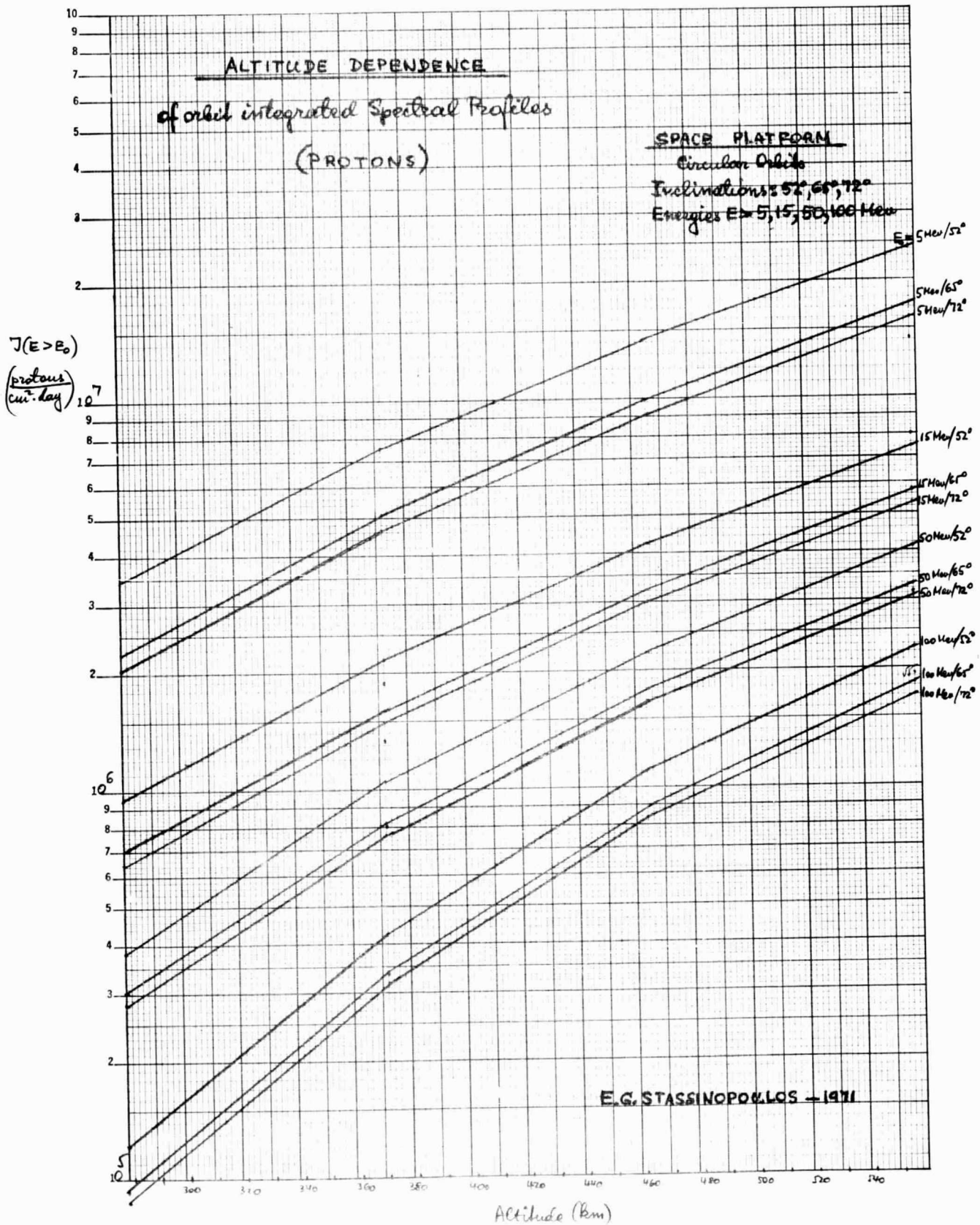
ALTITUDE DEPENDENCE
of orbit integrated Spectral Profiles
(PROTONS)
SPACE PLATFORM
Circular Orbits
Inclinations: 52°, 65°, 72°
Energies E> 5, 15, 50, 100 Mev
E> 5 Mev/52°
5 Mev/65°
5 Mev/72°
15 Mev/52°
15 Mev/65°
15 Mev/72°
50 Mev/52°
50 Mev/65°
50 Mev/72°
100 Mev/52°
100 Mev/65°
100 Mev/72°
J(E>E₀)
(protons / cm².day)
10⁷
10⁶
10⁵
300
310
340
360
380
400
420
440
460
480
500
520
540
Altitude (Km)
E.G. STASSINOPOULOS — 1971

Percent of total lifetime spent in high intensity regions of the Van Allen belts and percent of total daily flux accumulated during this time.-

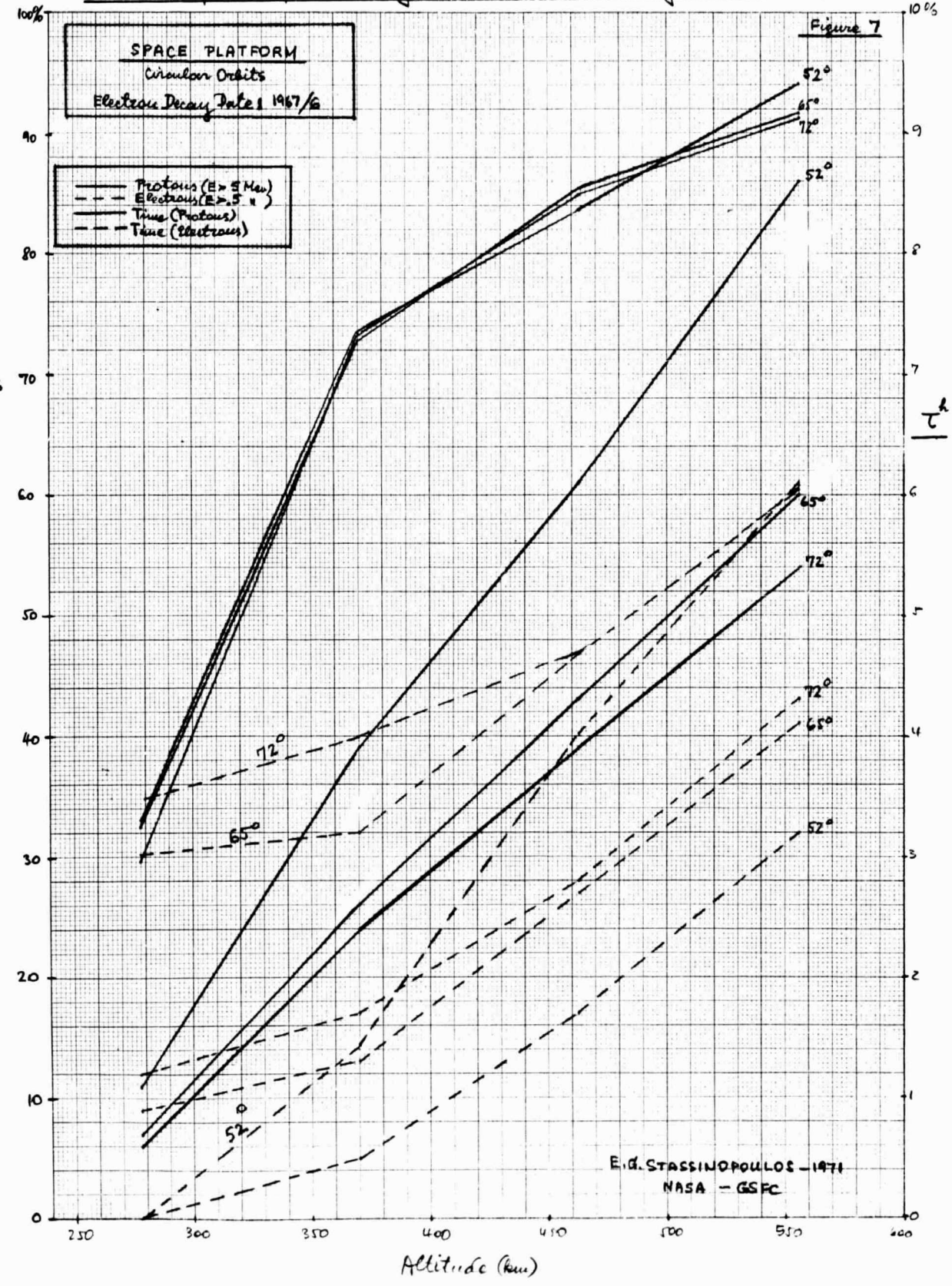

Percent of total lifetime spent in high intensity regions of the Van Allen belts and percent of total daily flux accumulated during this time --

Fig. 8

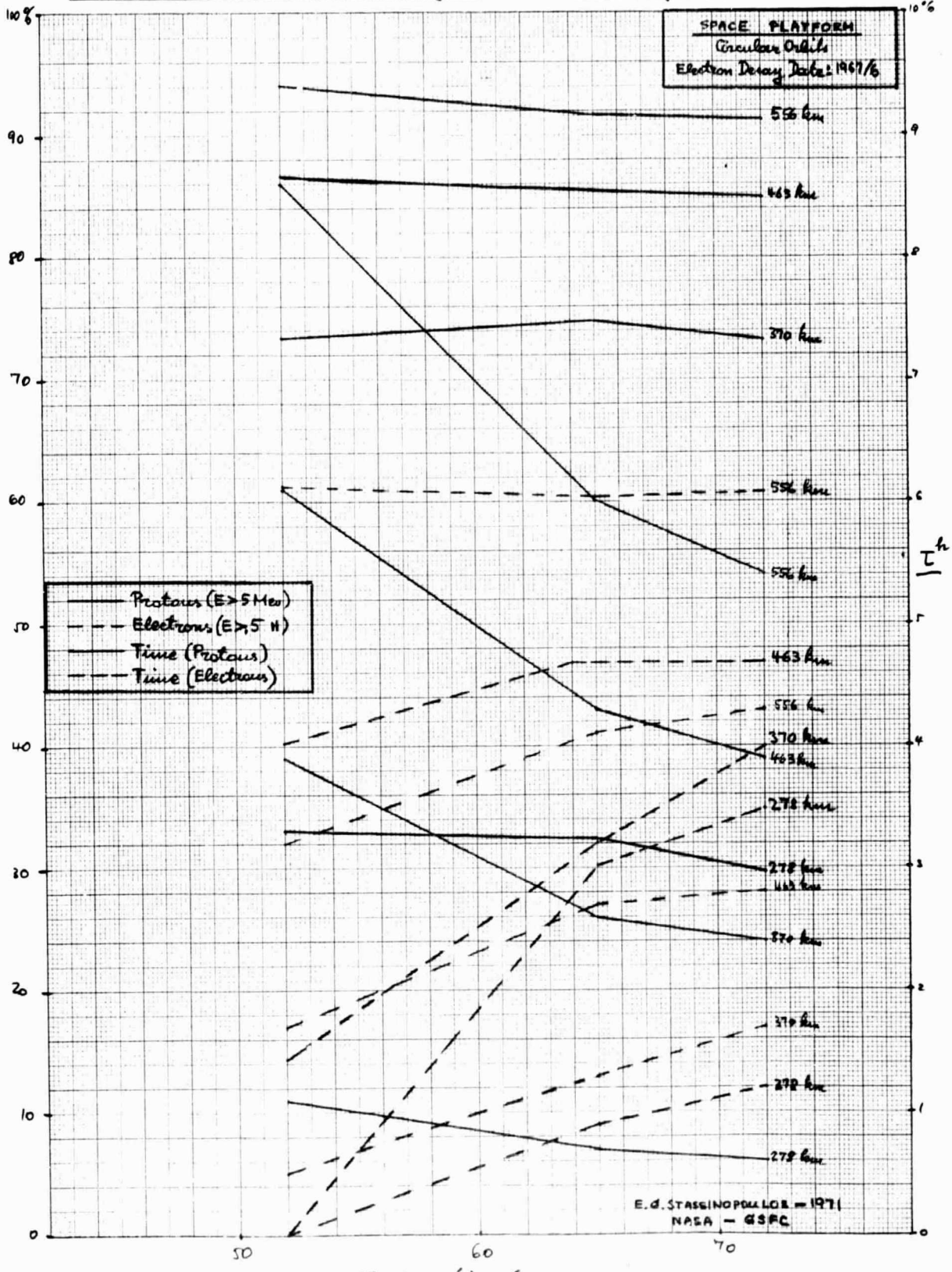

Figure 9

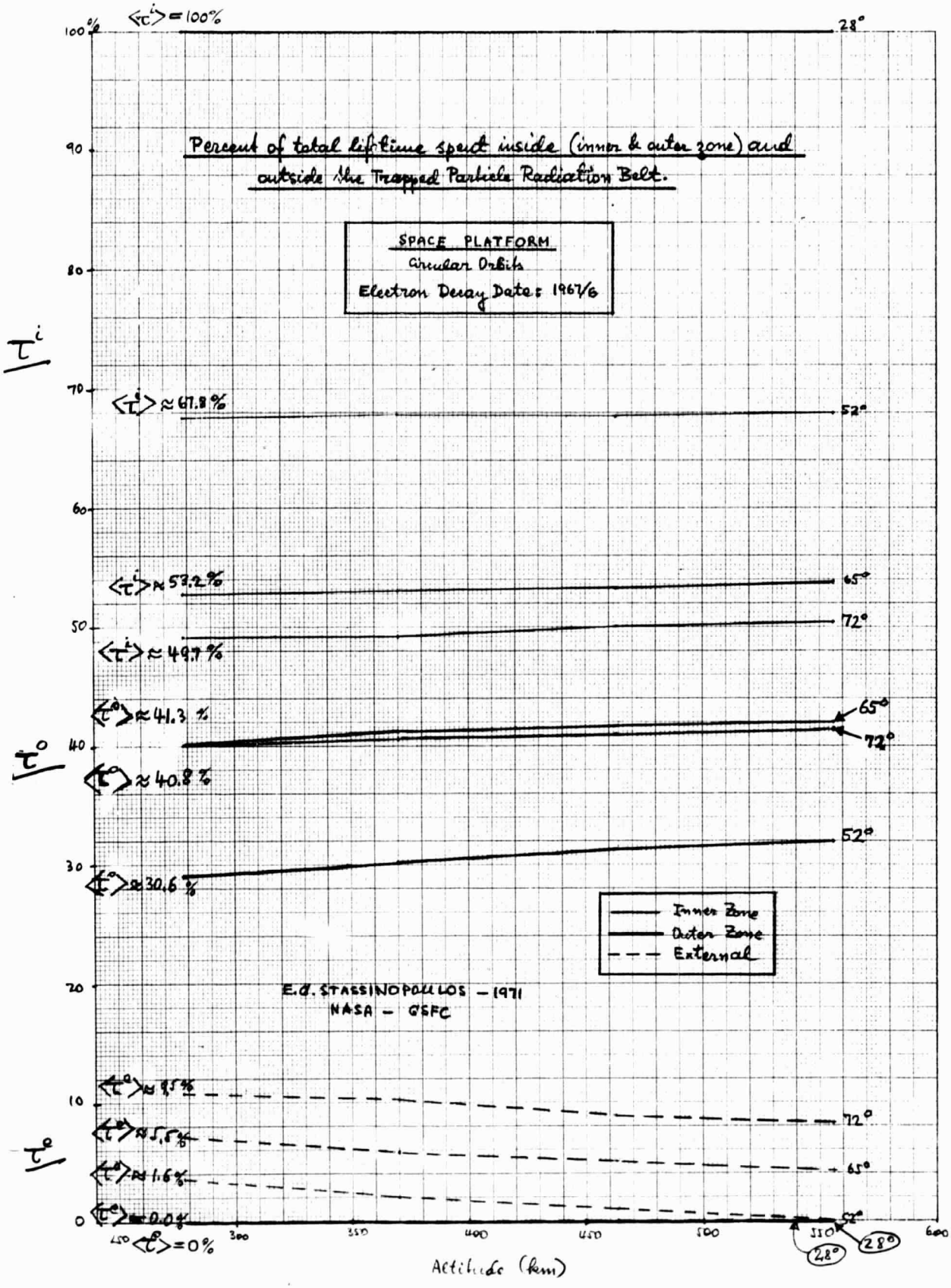
Percent of total lifetime spent inside (inner & outer zone) and outside the Trapped Particle Radiation Belt.
SPACE PLATFORM
Circular Orbits
Electron Decay Date: 1967/6
τ^i
τ^o
τ^e
$\langle\tau^i\rangle = 100\%$
28°
$\langle\tau^i\rangle \approx 61.8\%$
52°
$\langle\tau^i\rangle \approx 53.2\%$
65°
72°
$\langle\tau^i\rangle \approx 49.7\%$
$\langle\tau^o\rangle \approx 41.3\%$
65°
72°
$\langle\tau^o\rangle \approx 40.8\%$
52°
$\langle\tau^o\rangle \approx 30.6\%$
Inner Zone
Outer Zone
External
E.G. STASSINOPOULOS – 1971
NASA – GSFC
$\langle\tau^e\rangle \approx 9.5\%$
72°
$\langle\tau^e\rangle \approx 5.8\%$
65°
$\langle\tau^e\rangle \approx 1.6\%$
52°
$\langle\tau^e\rangle = 0.0\%$
$\langle\tau^e\rangle = 0\%$
28°
28°
100%
90
80
70
60
50
40
30
20
10
0
250
300
350
400
450
500
550
600
Altitude (km)

Percent of total lifetime spent inside (inner & outer zone) and outside the Trapped Particle Radiation Belt.

Figure 10

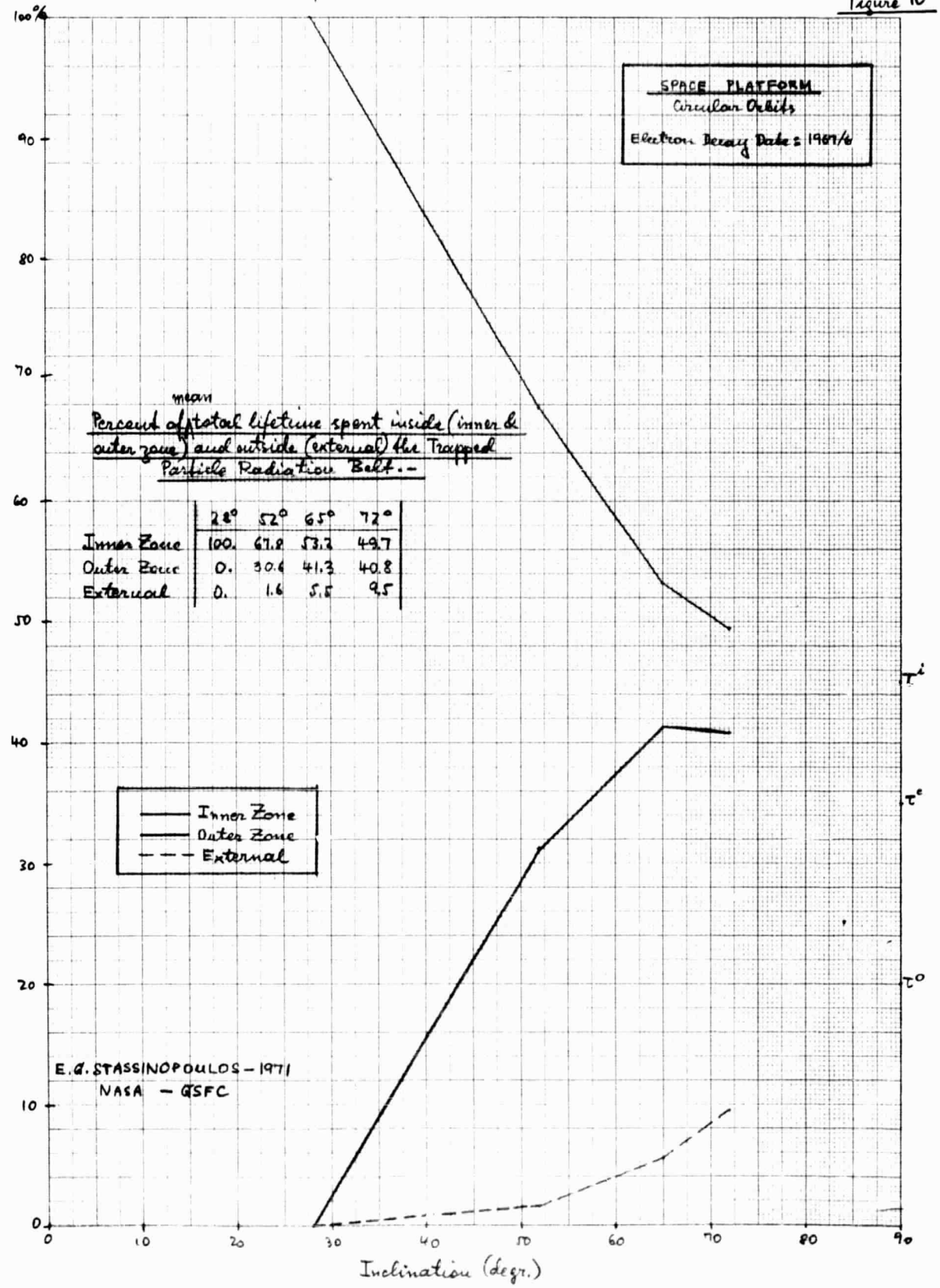

$\langle \tau \rangle$ = mean Percent of total lifetime spent inside (inner & outer zone) and outside (external) the Trapped Particle Radiation Belt.

	28°	52°	65°	72°
Inner Zone	100.	67.8	53.2	49.7
Outer Zone	0.	30.6	41.3	40.8
External	0.	1.6	5.5	9.5

Figure 11

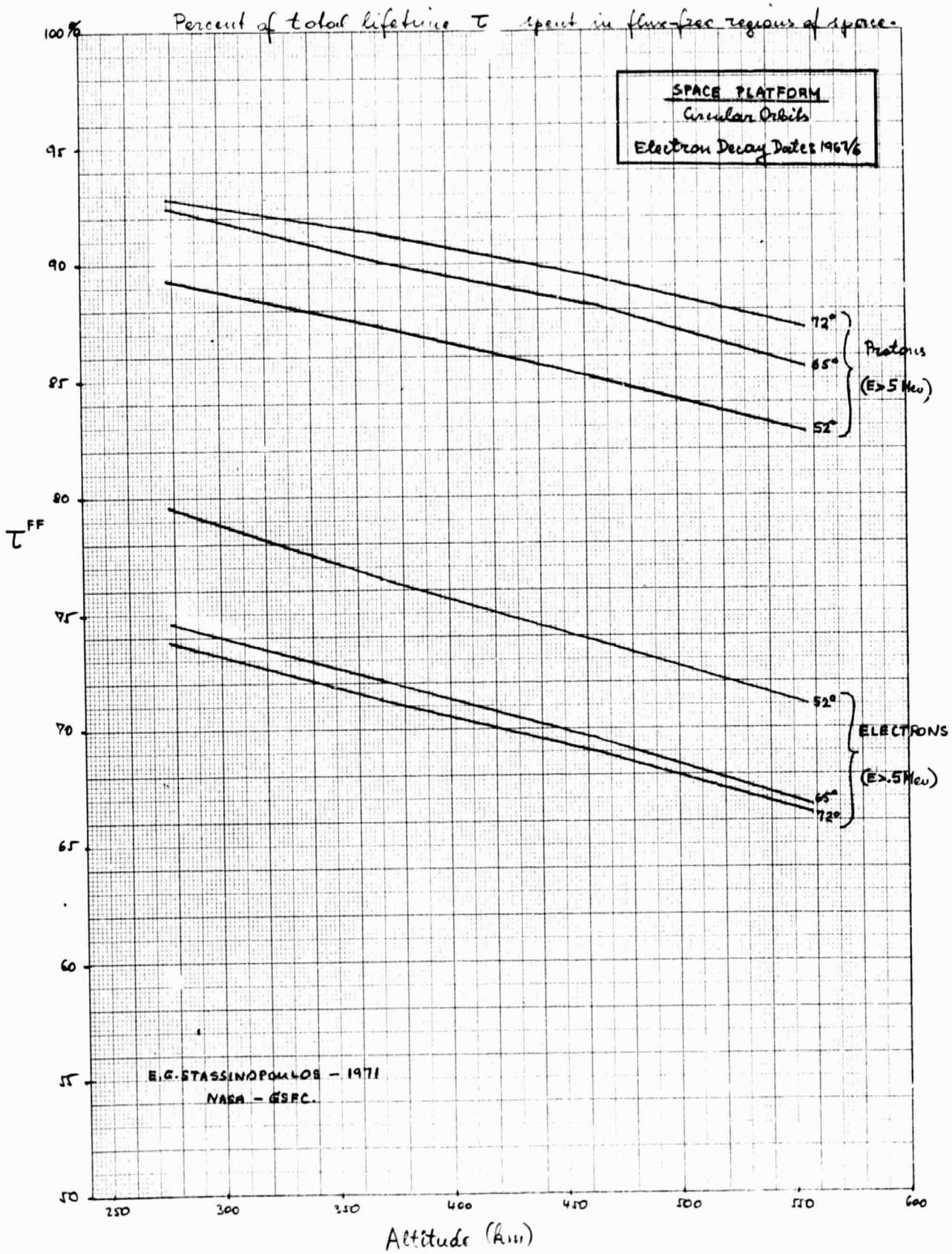
Percent of total lifetime τ spent in flux-free regions of space.
SPACE PLATFORM
Circular Orbits
Electron Decay Dates 1967/6
100%
95
90
85
80
75
70
65
60
55
50
τ^{FF}
72°
65°
52°
Protons
(E>5 Mev)
52°
65°
72°
ELECTRONS
(E>.5 Mev)
E.G. STASSINOPOULOS – 1971
NASA – GSFC.
250
300
350
400
450
500
550
600
Altitude (km)

Figure 12

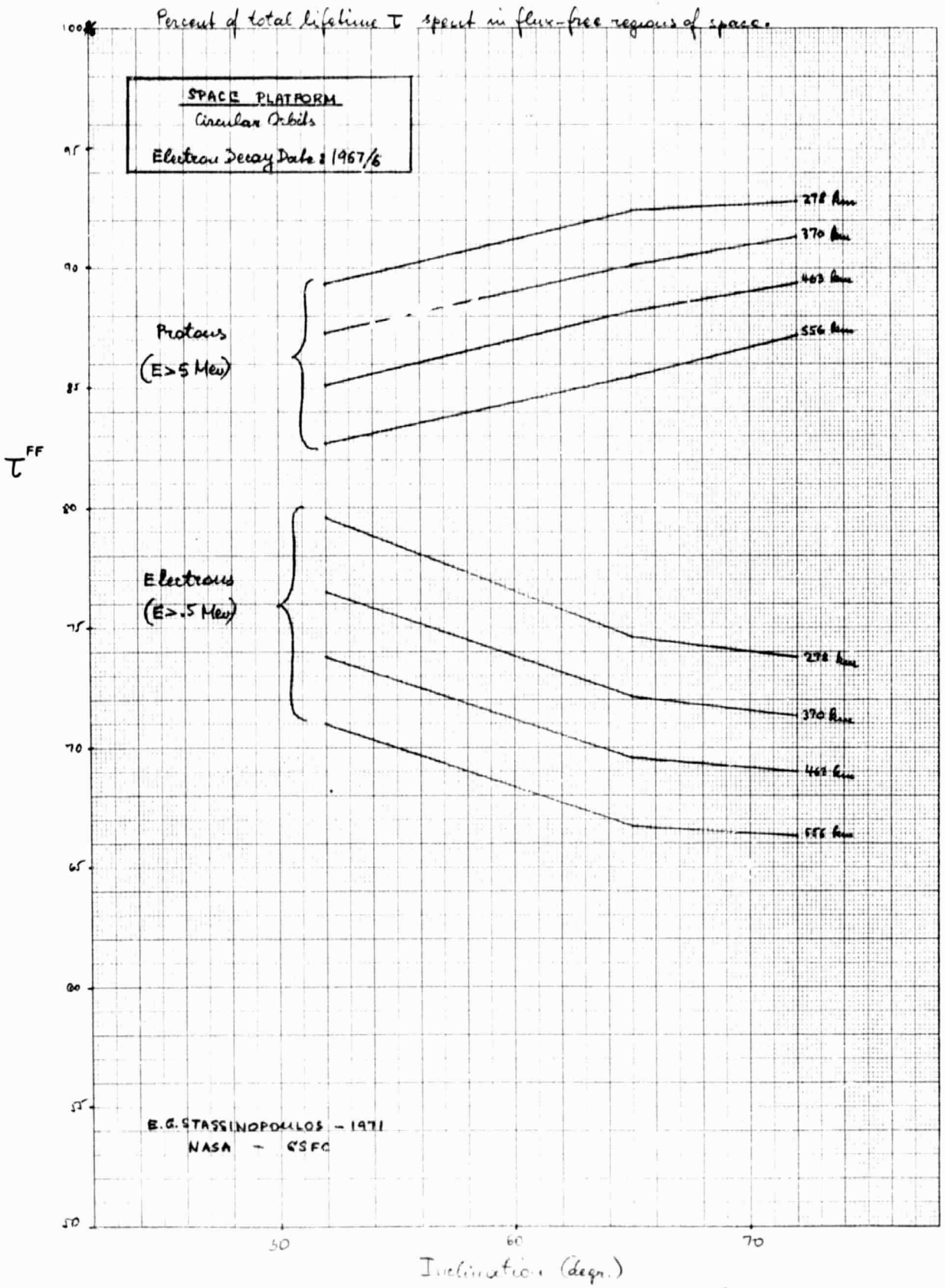
Percent of total lifetime τ spent in flux-free regions of space.
SPACE PLATFORM
Circular Orbits
Electron Decay Data : 1967/6
Protons
(E>5 Mev)
Electrons
(E>.5 Mev)
278 Km
370 Km
463 Km
556 Km
278 Km
370 Km
463 Km
556 Km
τ^{FF}
100%
95
90
85
80
75
70
65
60
55
50
50
60
70
Inclination (deg.)
B.G. STASSINOPOULOS – 1971
NASA – GSFC

TABLE 1

SPACE PLATFORM

ELECTRONS*

	E_o (Mev) \ i =	28°		52°		65°		72°	
		$J_e(E>E_o)$	%	$J_e(E>E_o)$	%	$J_e(E>E_o)$	%	$J_e(E>E_o)$	%
556 km:	.5	1.443^{9}	100	1.098^{9}	100.	1.367^{9}	100.	1.365^{9}	100.
	1	7.698^{8}	53.3	4.745^{8}	43.2	5.375^{8}	39.3	5.252^{8}	38.5
	3	6.861^{7}	4.75	3.899^{7}	3.55	3.406^{7}	2.49	3.167^{7}	2.32
	5	8.173^{6}	0.57	4.348^{6}	0.40	3.611^{6}	0.26	3.305^{6}	0.24
	7	1.009^{6}	0.07	5.194^{5}	0.05	4.302^{5}	0.03	3.902^{5}	0.03
463 km:	.5			6.109^{8}	100.	8.841^{8}	100.	9.026^{8}	100.
	1			2.474^{8}	40.5	3.225^{8}	36.5	3.224^{8}	35.7
	3			1.830^{7}	3.00	1.694^{7}	1.92	1.583^{7}	1.75
	5			1.959^{6}	0.32	1.654^{6}	0.19	1.503^{6}	0.17
	7			2293^{5}	0.04	1.915^{5}	0.02	1.723^{5}	0.02
370 km:	.5	1.299^{8}	100.	3.276^{8}	100.	5.945^{8}	100.	6.231^{8}	100.
	1	6.880^{7}	53.0	1.223^{8}	37.3	2.050^{8}	34.2	2.069^{8}	33.2
	3	6.085^{6}	4.68	8.262^{6}	2.52	8.311^{6}	1.39	7.889^{6}	1.27
	5	7.089^{5}	0.55	8.561^{5}	0.26	7.030^{5}	0.12	6.583^{5}	0.11
	7	8.734^{4}	0.07	1.000^{5}	0.03	7.743^{4}	0.01	7.271^{4}	0.01
278 km:	.5			1.811^{8}	100.	4.082^{8}	100.	4.388^{8}	100.
	1			6.074^{7}	33.5	1.329^{8}	32.6	1.399^{8}	31.9
	3			3.339^{6}	1.84	4.055^{6}	0.99	4.067^{6}	0.93
	5			3.156^{5}	0.17	2.708^{5}	0.07	2.626^{5}	0.06
	7			3.557^{4}	0.02	2.688^{4}	0.01	2.570^{4}	0.01

Spectral Distribution and Percentage of averaged, orbit integrated, vehicle encountered, omnidirectional, integral electron fluxes.—

Units: particles/cm^2.day

* The (inner zone) artificial component of the model environment has been decayed to 1967/6.—

E.G. STASSINOPOULOS – 1971
NASA – GSFC

TABLE 2

SPACE PLATFORM

PROTONS

Spectral Distribution and Percentage of averaged, orbit integrated, vehicle encountered, omnidirectional, integral proton fluxes. —

Units: particles/cm².day

	E_o(Mev) \ i =	28°		52°		65°		72°	
		$J_p(E>E_o)$	%	$J_p(E>E_o)$	%	$J_p(E>E_o)$	%	$J_p(E>E_o)$	%
556 km:	3	1.868^{7}	100	5.472^{7}	100	3.799^{7}	100	3.452^{7}	100
	5	1.419^{7}	76.0	2.426^{7}	44.3	1.736^{7}	45.5	1.596^{7}	46.2
	15	8.010^{6}	42.9	7.440^{6}	13.6	5.710^{6}	15.0	5.320^{6}	15.4
	50	5.366^{6}	28.7	4.111^{6}	7.5	3.289^{6}	8.7	3.072^{6}	8.9
	100	3.138^{6}	16.8	2.266^{6}	4.1	1.836^{6}	4.8	1.709^{6}	5.0
463 km:	3	—	—	3.391^{7}	100	2.266^{7}	100	2.049^{7}	100
	5	—	—	1.416^{7}	41.8	9.895^{6}	43.7	9.046^{6}	44.1
	15	—	—	4.233^{6}	12.5	3.219^{6}	14.2	2.993^{6}	14.6
	50	—	—	2.232^{6}	6.6	1.786^{6}	7.9	1.667^{6}	8.1
	100	—	—	1.118^{6}	3.3	8.963^{5}	4.0	8.411^{5}	4.1
370 km:	3	2.207^{6}	100	1.905^{7}	100	1.228^{7}	100	1.114^{7}	100
	5	1.876^{6}	85.0	7.504^{6}	39.4	5.058^{6}	41.2	4.630^{6}	41.6
	15	1.333^{6}	60.2	2.162^{6}	11.4	1.605^{6}	13.1	1.492^{6}	13.4
	50	8.049^{5}	21.3	1.036^{6}	5.4	8.229^{5}	6.7	7.665^{5}	6.9
	100	3.358^{5}	15.2	4.259^{5}	2.2	3.392^{5}	2.8	3.159^{5}	2.8
278 km:	3	—	—	9.472^{6}	100	5.813^{6}	100	5.254^{6}	100
	5	—	—	3.449^{6}	36.4	2.254^{6}	38.8	2.055^{6}	39.1
	15	—	—	9.499^{5}	10.0	6.997^{5}	12.0	6.457^{5}	12.3
	50	—	—	3.808^{5}	4.0	3.021^{5}	5.2	2.807^{5}	5.3
	100	—	—	1.232^{5}	1.3	9.185^{4}	1.6	8.782^{4}	1.7

E.G. STASSINOPOULOS — 1971
NASA — GSFC

TABLE 3

SPACE PLATFORM

Percent of total Lifetime spent in High Intensity ⊕ regions of the Radiation Belts and percent of total daily Flux accumulated during this time.

PROTONS (E>5 Mev):		28°	52°	65°	72°	ELECTRONS (E>.5 Mev)*:	28°	52°	65°	72°
556 km:										
	% Time	6.0	8.6	6.0	5.4		3.7	3.2	4.1	4.3
	% Flux	86.9	94.1	91.7	91.3		88.4	61.3	60.4	60.7
463 km:										
	% Time	—	6.1	4.3	3.9		—	1.7	2.7	2.8
	% Flux	—	83.6	85.4	84.9		—	40.2	46.8	46.9
370 km:										
	% Time	.04	3.9	2.6	2.4		0.2	0.5	1.3	1.7
	% Flux	1.6	73.4	72.8	73.2		12.6	14.3	32.1	39.9
278 km:										
	% Time	—	1.1	0.7	0.6		—	0.0	0.9	1.2
	% Flux	—	33.0	32.4	29.6		—	0.0	30.2	34.9

⊕ "High Intensity" are defined those regions of the Trapped Particle Radiation Belts, where positional, instantaneous, integral, omnidirectional, vehicle encountered fluxes exceed:

a) 10^3 particles $cm^{-2} sec^{-1}$ for protons with energies E > 5 Mev.

b) 10^5 particles $cm^{-2} sec^{-1}$ for electrons with energies E > .5 Mev

* The (inner-zone) artificial component of the model environment has been decayed to 1967/6.—

E.G. STASSINOPOULOS — 1971
NASA — GSFC

TABLE 4

SPACE PLATFORM

Percent of total Lifetime spent inside (inner and outer zone) and outside the Trapped Particle Radiation Belt.-

		28°	52°	65°	72°	
556 km:						
Inside	Inner Zone	100.0	68.0	53.8	50.4	τ^i
	Outer Zone	—	32.0	42.0	41.4	τ^o
Outside		—	—	4.2	8.2	τ^e
463 km:						
Inside	Inner Zone	*	67.7	53.3	50.1	τ^i
	Outer Zone	*	31.3	41.7	41.0	τ^o
Outside		*	1.0	5.0	8.9	τ^e
370 km:						
Inside	Inner Zone	100.0	67.8	53.0	49.2	τ^i
	Outer Zone	—	30.2	41.2	40.6	τ^o
Outside		—	2.0	5.8	10.2	τ^e
278 km:						
Inside	Inner Zone	*	67.5	52.8	49.1	τ^i
	Outer Zone	*	29.0	40.1	40.1	τ^o
Outside		*	3.5	7.1	10.8	τ^e

E. G. STASSINOPOULOS – 1971
NASA – GSFC

* No calculations performed

TABLE 5

SPACE PLATFORM

Percent of Total Lifetime spent in Flux-Free⊕ regions of Space

PROTONS (E>5 Mev):	28°	52°	65°	72°	ELECTRONS (E>.5 Mev)*:	28°	52°	65°	72°
556 km	82.7	82.7	85.5	87.2		83.3	71.0	66.7	66.3
463 km	—	85.1	88.2	89.4		—	73.8	69.6	69.0
370 km	89.7	87.3	90.1	91.3		87.0	76.5	72.1	71.3
278 km	—	89.3	92.4	92.8		—	79.6	74.6	73.8

⊕ "Flux Free", in the context of this study, connotes intensities of less than one trapped particle $cm^{-2} sec^{-1}$ having the indicated energies, in accordance with the current environment models used. —

* The (inner-zone) artificial component of the model environment has been decayed to 1967/6. —

E.G. STASSINOPOULOS - 1971
NASA - GSFC